Processing Radio Plasma Imager Plasmagrams Utilizing Hierarchical Segmentation

I. A. Galkin, G. Khmyrov
and B. W. Reinisch
University of Massachusetts
Lowell, MA

J.C. Tilton and S. F. Fung

NASA Goddard Space Flight Center
Greenbelt, MD

***Abstract*— The Radio Plasma Imager (RPI) on the IMAGE spacecraft provides valuable information on the remote and local electron densities in the Earth's magnetosphere. This information is derived from the RPI plasmagrams, a common visual representation of active radio-sounding data in the format of echo intensity as a function of echo delay time (ordinate) and sounding frequency (abscissa). Due to the large volume of the archived RPI plasmagram imagery, automated data exploration software, "Cognitive Online Rpi Plasmagram Ranking Algorithm" (CORPRAL), has been developed to identify plasmagrams containing signatures of interest. CORPRAL routinely scans the RPI mission database to select qualifying plasmagrams. The echo detection algorithms implemented in the CORPRAL, still yield significant "false-alarms" and thus can benefit from the assistance of additional image processing techniques. As a NASA CICT/IDU Technology Infusion task, we are exploring the adaptation and incorporation of the recursive hierarchical segmentation (RHSEG) technique that was developed for a broad class of remotely sensed images of the Earth. The RHSEG algorithm iteratively builds a hierarchy of image segmentations of various detail levels using a hybridization of region growing, and constrained spectral clustering. Analysis of the segmentation hierarchy allows one to track the characteristics of each region in the process of its growing to optimally select the best segmentation level to describe the corresponding feature. Treatment of plasmagrams with the RHSEG will then provides good candidate signatures for registration, thus improving the robustness of CORPRAL. This paper discusses our progress to date.**

I. Introduction

THE Imager for Magnetopause-to-Aurora Global Exploration (IMAGE) satellite [2], launched in March 2000, is in a polar orbit with apogee of about 7 R_E altitude where it is well situated to observe the structure and dynamics of the Earth's magnetosphere during geomagnetic storms and the changes in the local plasma using the Radio Plasma Imager (RPI) [1]. The RPI instrument consists of a radio transmitter, receiver, and 3-axis antenna systems. Like radar, RPI transmits short, phase-coded pulses of electromagnetic waves that propagate to remote plasma regions and detects the reflected pulses as echoes. RPI is the first instrument to use radar echo techniques to measure remote magnetospheric densities along with natural noise and other emissions.

This work was supported by the Intelligent Systems project under NASA's CICT program. Work by the University of Massachusetts Lowell was performed under NASA Grant NAG5-13387. Work by J. C. Tilton was also supported by Intelligent Systems project NRA2-37143.

The RPI instrument on IMAGE is currently obtaining radio remote-sensing data about the density distribution of magnetospheric plasmas. RPI's chief product is the plasmagram, as shown in Fig. 1. The figure shows received signal strength (color scale) as a function of echo delay (range in vertical scale) and radio-sounder frequency (horizontal scale) of the radar pulses. The echoes observed above 500 kHz in Fig 1. are ducted echoes from within the Earth's plasmasphere. The vertical intensification near 400 kHz is a locally excited resonance. This resonance contains information about the local plasma density, while the echoes contain information about magnetic field aligned densities away from the spacecraft. Radar echoes from and within important magnetospheric structures, such as the magnetopause and the plasmapause, appear as traces on plasmagrams [9-13].

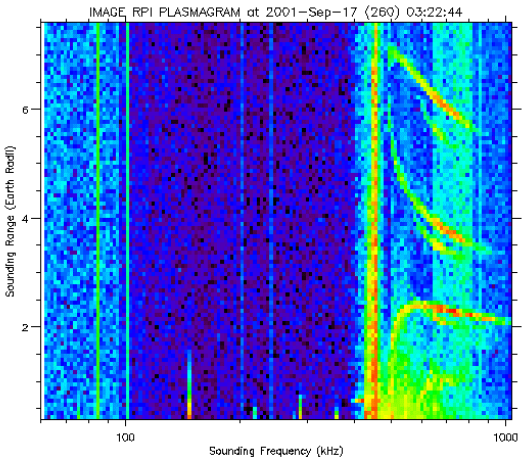

Fig. 1. IMAGE RPI Plasmagram at 03:22:33 on Sep. 17, 2001, designated 20010917_032244.

Less than 20% of all plasmagrams contain echo traces because RPI is a radar of opportunity whose signal reflects at a remote location and returns to the spacecraft location only sporadically on any particular orbit. The need to search for useful information in the IMAGE/RPI mission database holding 900,000 plasmagram images has been the rationale for development of automated techniques for data exploration

and signature characterization.

II. CORPRAL

Cognitive Online Rpi Plasmagram Ranking Algorithm (CORPRAL) [3,4] is an automated RPI data exploration system developed to identify plasmagrams containing signatures of interest. The signature recognition approach in the CORPRAL is best described as "biologically plausible" as it uses a model of the early (pre-attentive) vision system in mammals that "pops up" visual cues in the field of view without willful concentration of attention. The early vision can be described as a task that runs in the background and requests switch of attention to objects that present potential danger or special interest. This system is especially effective in rapid detection of salient objects by identifying their contours. Existing studies of the pre-attentive vision suggest that it implements a "bottom up" processing of visual information, where the raw image undergoes multiple stages of transformations in eye retina and cortical networks of the brain. Because each stage extracts elements of higher perceptual strength from its input, this model is often referred to as Marr's pyramid of perception [16].

The core of the plasmagram processing algorithm is a recurrent neural network that seeks the optimal state of dynamic system of interacting *rotors*, edge elements found by locating sharp intensity gradients in the plasmagram image and evaluating their local orientation. Fig.2 illustrates intermediate and final steps of CORPRAL analysis of the plasmagram in Fig.1.

The founding principle of the pre-attentive vision model designed for the CORPRAL analysis is collective interaction of rotors under Gestalt perceptual restrictions [14] of good continuation, smoothness, co-circularity and proximity. In the iterative process of this interaction, rotors align tangential to existing echo traces (as shown in middle panel of the Fig.2). This iterative process is best described in terms of the energy minimization, and in our case is accomplished by a feed-back optimizing neural network evolving into the global minimum of its energy. The starting configuration of rotors is obtained by finding edgel elements (edgels), sharp gradients of image intensity that are typical for object boundaries, and evaluating their local orientation. Once the rotors are optimally aligned to the traces, they are grouped in trace segments by a bottom-up clustering algorithm driven by a grouping criterion that considers alignment and proximity of rotors. Finally, the found segments are subjected to higher-level perceptual grouping analysis that may combine together segments belonging to the same trace. The grouping algorithm evaluates connection scores for all pairs of candidate segments. The score considers length and smoothness of a line connecting the gap between the trace segments. The lower panel of Fig. 2 shows seven traces found by CORPRAL in the plasmagram shown in Fig.1.

To reduce computational demand of the optimization problem of collective rotor interaction, we introduced a

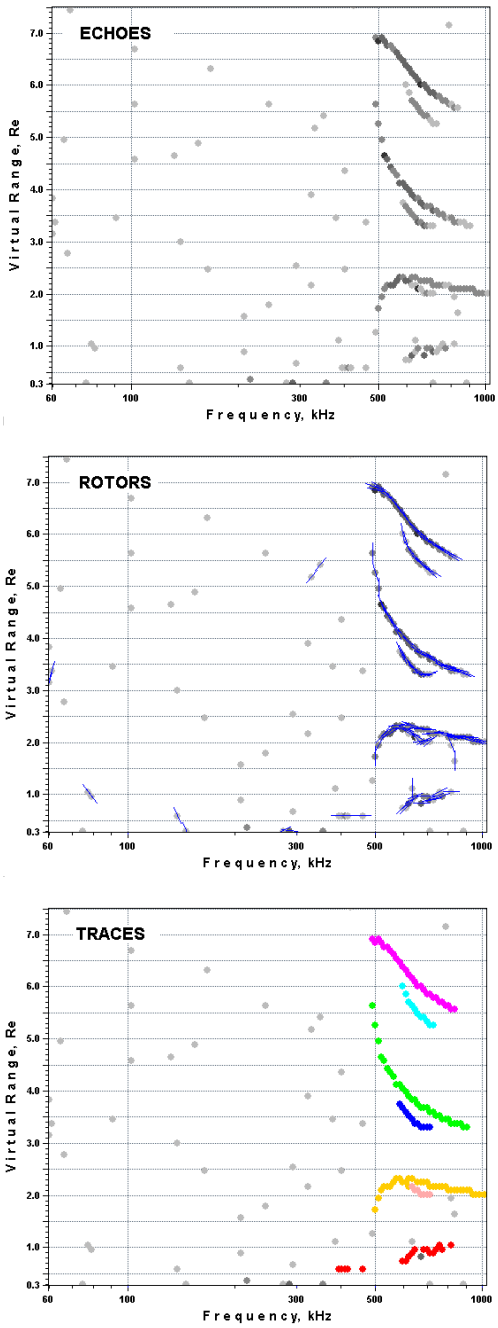

Fig. 2. CORPRAL processing results for the plasmagram in Fig.1. (Top to bottom): detected echoes, optimized rotor orientations, and found traces.

thresholding algorithm that removes noise background prior to localization of edge elements. The noise pixels are identified using the echo detection principle commonly used in radar and remote sensing operations. The present version of the CORPRAL software uses an adaptive thresholding algorithm that evaluates the local noise level using a 1D sliding analysis window placed vertically on the plasmagram.

The CORPRAL analysis is performed on the plasmagram images in the RPI mission database at UMass Lowell as soon

as they arrive for ingestion from the IMAGE Space Mission Operating Center at Goddard SFC. Plasmagrams tagged for the presence of traces (presently over 145,000) are available for queries from the RPI BinBrowser data visualization platforms [15].

As analysis of the CORPRAL performance shows, the thresholding technique in its present implementation causes a noticeable "false-alarm" rate. As a NASA CICT/IDU Technology Infusion task, we are exploring the adaptation and incorporation of the recursive hierarchical segmentation (RHSEG) technique [5] as a technique for improving echo detection algorithm, or in the capacity of a full-featured trace extraction technique.

III. Recursive Hierarchical Segmentation

Recursive hierarchical segmentation (RHSEG) [5], [6] is being investigated as an approach for reducing the number of "false-alarms" produced by CORPRAL. RHSEG is a recursive formulation of hierarchical segmentation (HSEG), which is a hybrid of hierarchical step-wise optimization (HSWO) [7] and constrained spectral clustering that produces a hierarchical set of image segmentations based on detected convergences. HSWO is an iterative approach to region growing in which the optimal image segmentation as measured by a dissimilarity function is found at *N*-1 regions, given a segmentation at *N* regions. The initial segmentation at *N* regions can be provided by some other segmentation procedure or may be defined by labeling each image pixel as a single pixel region. The iterative process continues until stopped by some stopping criterion (defined later in this section). HSEG optionally interjects between HSWO iterations merges of spatially non-adjacent regions (i.e., spectrally based merging or clustering) constrained by a threshold derived from the previous HSWO iteration, and includes an approach for selecting segmentations from particular iterations to save as a final segmentation hierarchy result. While the addition of constrained spectral clustering improves the segmentation results, especially for larger images, it also significantly increases HSEG's computational requirements. To counteract this, a computationally efficient recursive implementation of HSEG (RHSEG) has been devised [5]. Included in this implementation is special code that is required to avoid processing window artifacts caused by RHSEG's recursive subdivision and subsequent recombination of the image data.

A. HSEG Algorithm[6]:

1) Give each image pixel a region label and set the global dissimilarity value, dval, equal to zero. If a pre-segmentation is provided, label each image pixel according to the pre-segmentation. Otherwise, label each image pixel as a separate region.
2) Calculate the dissimilarity value, dissim_val, between all pairs of spatially adjacent regions. If spclust_wght > 0.0, also calculate dissim_val for spatially non-adjacent regions.
3) Find the smallest dissim_val between spatially adjacent pairs of regions and set the value of the maximum merging threshold, max_threshold, equal to it.
4) If spclust_wght equals zero, go to step 7. Otherwise, merge all pairs of regions (spatially adjacent or spatially non-adjacent) with dissim_val = 0.0 or dissim_val < spclust_wght*max_threshold.
5) If the number of regions remaining is less than or equal to the preset value conv_nregions, go to step 11. Otherwise, update the dissim_val's between spatially adjacent pairs of regions as necessary.
6) Find the smallest dissim_val between spatially adjacent pairs of regions and set threshold equal to it. If threshold > max_threshold, set max_threshold = threshold.
7) Merge all pairs of spatially adjacent regions with dissim_val ≤ max_threshold. (Update the dissim_val's for spatially adjacent regions between each merge as necessary.)
8) If the number of regions remaining is less than or equal to the preset value conv_nregions, go to step 11, or if spclust_wght equals zero, go to step 11. Otherwise, update the dissim_val's between all pairs of spatially adjacent and non-adjacent regions.
9) Merge all pairs of spatially adjacent or non-adjacent regions with dissim_val ≤ spclust_wght*max_threshold. (For the most part, only spatially non-adjacent merges will occur. Update the dissim_val's for spatially adjacent and non-adjacent regions between each merge as necessary.)
10) If the number of regions remaining is less than or equal to chk_nregions, go to step 11. Otherwise, go to step 6.
11) If the number of regions remaining is less than or equal to conv_nregions, save the current region label map to disk along with associated region information and STOP. Otherwise, let prev_dval = dval, calculate the current global dissimilarity value, and set dval equal to this value. If prev_dval = zero, save the current region label map to disk along with associated region information, and go to step 6. Otherwise, calculate dratio = dval/prev_dval. If dratio is greater than the preset threshold convfact, save the region label map from the previous iteration to disk along with associated region information, and go to step 6. Otherwise, just go to step 6.

Note that *spclust_wght*, *chk_nregions*, *convfact*, and *conv_nregions* are user specified parameters. If *spclust_wght* = 0.0, HSEG is essentially identical to HSWO with convergence checking (step 11) for segmentation hierarchy selection. The associated region information mentioned in step 11 above is the region number of pixels list, and optionally includes the boundary region map, the region number of boundary pixels list, the region mean vector list, the region standard deviation list, and the region criterion value list (the portion of the global dissimilarity value contributed by each region).

B. Recursive HSEG (RHSEG) Algorithm[5]:

1) Given an input image X, specify the number levels of recursion required (rnb_levels) and pad the input image, if necessary, so that the width and height of the image can be evenly divided by $2^{nblevels-1}$. (A good value for rnb_levels results in an image section at level = rnb_levels consisting of roughly 1000 to 4000 pixels.) Set level = 1.
2) Call rhseg(level,X).
3) Execute the HSEG algorithm (per part A this section) on the image X using as a pre-segmentation the segmentation output by the call to rhseg( ) in step 2.

where rhseg(*level*,*X*) is as follows:

1) If *level* = *rnb_levels*, go to step 3. Otherwise, divide the image data into quarters (i.e., half the width and height dimensions) and call rhseg(*level*+1,*X*/4) for each image quarter (represented as *X*/4).
2) After all four calls to rhseg() from step 1 complete processing, reassemble the image segmentation results.
3) If *level* < *rnb_levels*, initialize the segmentation with the reassembled segmentation results from step 2. Otherwise, initialize the segmentation with one pixel per region. Execute the HSEG algorithm (per part A this section) on the image *X* with the following modification: Terminate the algorithm when the number of regions reaches the preset value *min_nregions*.
4) If *level* = *rnb_levels*, exit. Otherwise, find the regions that are likely to contain pixels that are more similar to one or more other regions. This is done through examining pairs of regions that border each other along the processing window seam between the four reassembled sections of image data and pairs of regions that are spectrally similar to each other. Then, for these pairs of regions, swap region assignments of pixels that are *switch_pixels_factor* more similar to the other region (generally *switch_pixels_factor* > 1.0 to prevent excessive switching of pixel region assignments). This process is described in more detail in [8] (which was used as the basis for a recent patent application). After the completion of this region assignment swapping process, exit.

Note that *rnb_levels*, *switch_pixels_factor*, and *min_nregions* are user specified parameters.

If *max_npixels* is the product of the number of row and columns in the recursively subdivided image data at the deepest level of recursion, the number of spatially non-adjacent regions that need to be compared in step 4 of HSEG is less that the greater of *max_npixels* and 4**min_nregions*. This significantly reduces the computational burden.

The region assignment swapping procedure outlined in step 4 of *rhseg*( ) is necessary because, especially when processing image larger than 512x512, processing window artifacts are often seen in the image segmentation results along the seams between the recursively subdivided and reassembled image portions, unless this region assignment swapping process is carried out. The region assignment swapping process is very efficient and adds very little overhead (less than 10%) to the computation requirements.

Since the region assignment swapping procedure can introduce spatially non-connected regions, when RHSEG is utilized with no spectral clustering (i.e., *spclust_wght* = 0.0), connected component labeling must be run on the resulting region labeling to restore the spatial connectivity of the regions. Since this will generally result in an increase in the number of regions, the HSEG algorithm must be again run on the connected component labeling result until the segmentation reaches the number of regions specified in step 3 (*min_nregions*, or if *level* = 1, the greater of *min_nregions* or *chk_nregions*). The connected component labeling and rerunning of the HSEG algorithm can substantially increase the processing time required. Note that RHSEG run with no spectral clustering is effectively a recursive version of HSWO.

IV. Region Merge and Global Dissimilarity Criterion:

Several different region merge dissimilarity criteria can be used with RHSEG (see [5] and [6]). This study uses the "mean squared error" (*MSE*) dissimilarity criterion [6]:

$$d_{MSE}(X_i, X_j) = \frac{n_i n_j}{(n_i + n_j)} (\mu_i - \mu_j)^2, \qquad (1)$$

where X_i (X_j) is the subset of the image *X* corresponding to region *i* (*j*), n_i (n_j) is the number of pixels in region *i* (*j*), and μ_i (μ_j) is the mean value of region *i* (*j*).

Likewise, several different global dissimilarity can be used. This study uses the "mean squared error" (*MSE*) global dissimilarity criterion [6]:

$$D_{MSE}(X) = \frac{1}{(M-1)} \sum_{i=1}^{N} \sum_{x_p \in X_i} (\chi_p - \mu_i)^2, \qquad (2)$$

where χ_p is an image pixel value, *N* is the number of regions, and *M* is the number of pixels in image *X*.

V. Plasmagram Analysis using RHSEG

A. Plasmagram 20010917_032244:

To gain an understanding of the behavior of RHSEG in analyzing RPI plasmagrams, several plasmagrams have been studied. To avoid early discouragement, an admittedly easy plasmagram was chosen for initial analysis: IMAGE RPI Plasmagram at 03:22:44 on Sep. 17, 2001 (Fig. 1), designated 20010917_032244.

The first thing to be noted about this plasmagram is that there are only 76 distinct data values in it. This means that ANY segmentation approach that allows non-adjacent regions to merge will produce the same 76 region segmentation with a zero threshold.

RHSEG was initialized from the zero threshold 76 region segmentation and run on plasmagram 20010917_032244 with *rnb_levels* = 1, *spclust_wght* = 1.0, *convfact* = 1.1, and *conv_nregions* = 2. Convergence checking was initiated

immediately at the 76 region point (*chk_nregions* = 76).

Major jumps in *dval* and *max_threshold* were noticed between hierarchical level 10 (66 regions, *dval* = 0.0901673, and *max_threshold* = 20.0357) and hierarchical level 11 (10 regions, *dval* = 2.02209, and *max_threshold* = 11524.2). RHSEG was then rerun with *chk_nregions* = 10, and the 10 region segmentation result was inspected with the *HSEGViewer* visualization tool, which is specifically designed to inspect and manipulate the results obtained form HSEG and RHSEG.

Starting at the 10 region segmentation, RHSEG produced a segmentation hierarchy consisting of eight hierarchical levels. The segmentation at the first hierarchical level has 10 regions in it and the segmentation at the second hierarchical level has 9 regions in it. In other words, eight of the regions at the second hierarchical level are identical to the regions at the first hierarchical level, while one region at the second hierarchical is formed by the merge of a pair of regions at the first hierarchical level. The other six hierarchical levels (after the first two) have 8, 7, 6, 5, 4 and 2 regions in them, respectively. The segmentations at the coarser levels of the segmentation hierarchy are formed from selective merges of pairs of regions in the segmentations at the finer levels of the segmentation hierarchy.

Fig. 3 shows a color coded result of the RHSEG segmentation result. Regions 4, 5, 7, 8 and 10 at the finest segmentation hierarchy level eventually merge going down the segmentation hierarchy to form one region at the coarsest level of the segmentation hierarchy. These regions were seen to form the lower data value background (blue in Fig. 3). Regions 2, 6 and 9 at the finest segmentation hierarchy level eventually merge going down the segmentation hierarchy to form one region at hierarchical level 7 (the second coarsest level). These regions were seen to form the intermediate level background (tourquoise in Fig. 3). Regions 1 and 3 at the finest segmentation hierarchy level also merge going down the segmentation hierarchy to form on region at hierarchical level 7. These regions contain the plasma resonances and trace signals (color coded pink in Fig. 3).

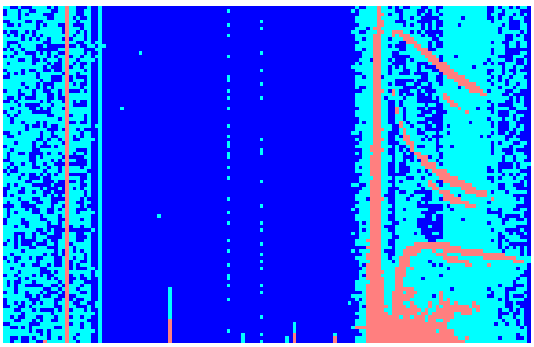

Fig. 3. Initial result from RHSEG. Three regions were selected with the *HSEGViewer* program: Low value background (blue), intermediate value background (tourquiose), and signal (pink).

Shape descriptors under investigation should allow the automatic extraction of the regions corresponding to the resonance and trace signals (work in progress). Shape descriptors being sought are mathematical constructs that can indicate whether or not a region is elongated, and in which direction. An elongated region at a constant frequency would indicate a plasma resonance. An elongated region at varying frequency would indicate a plasma trace.

A mask was created with regions 1 and 3 from the initial result from RHSEG, and RHSEG was rerun with this mask and the same parameters as before, with the exception of *spclust_wght* = 0.0, and *convfact* = 1.02. Major jumps in *dval* and *max_threshold* were noticed between hierarchical level 9 (27 regions, *dval* = 4.8965, and *max_threshold* = 600.333) and hierarchical level 10 (24 regions, *dval* = 5.1304, and *max_threshold* = 1128.53). RHSEG was then rerun with *chk_nregions* = 24, and the 24 region segmentation result was inspected with the *HSEGViewer* visualization tool.

Regions 18, 19, and 24 were seen to form part of the background (grayish-blue), regions 17, 21, 22 and 23 make of regions corresponding to resonance signals (shades of brown), and trace signals were found in regions 10, 11, 12, 13, 14, 15, 16 and 20 (other colors). Regions 1-8 (each having less than eight data points) were left unlabeled (black). The masked out area is grey. The color coded result is displayed in Fig. 4.

Again, shape descriptors under investigation should allow the automatic extraction of the regions corresponding to the resonance and trace signals (work in progress).

B. Plasmagram 20010118_023716:

A second test was performed on the IMAGE RPI Plasmagram at 02:37:16 on Jan. 18, 2001 (Fig. 5), designated 20010118_023716. Again, the first thing to be noted about this plasmagram is the limited number of distinct data values. Since there are only 62 distinct data values, any segmentation approach that allows non-adjacent regions to merge will produce the same 62 region segmentation with zero threshold.

RHSEG was initialized from the zero threshold 62 region segmentation and run on plasmagram 20010118_23716 with

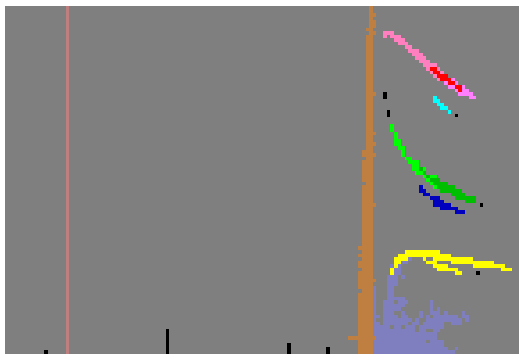

Fig. 4. Final result from RHSEG. Three regions were selected with the *HSEGViewer* program: Background (grey and greyish-blue), unlabeled (black), resonance signals (shades of brown), and trace signals (other colors).

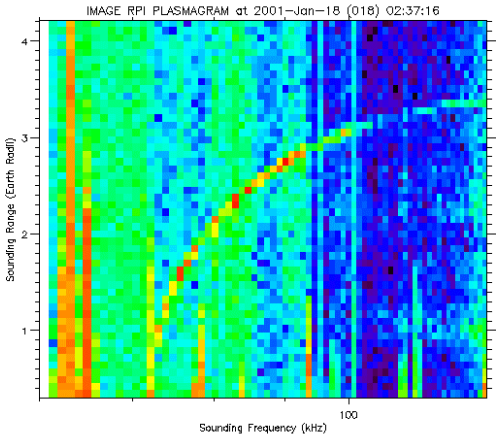

Fig. 5. IMAGE RPI Plasmagram at 02:37:16 on Jan. 18, 2001, designated 20010118_023716.

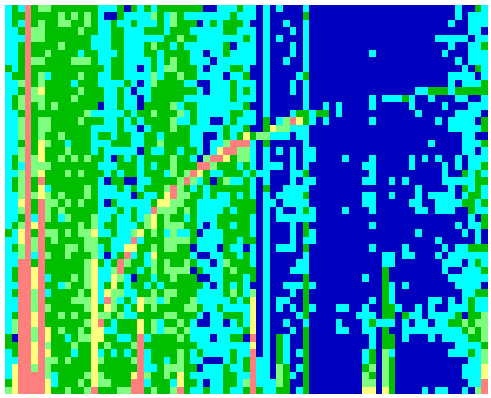

Fig. 6. Colored coded initial segmentation result from RHSEG. Regions are colored coded to closely match the pseudo coloring used in Fig. 5 to display the input data.

rnb_levels = 1, *spclust_wght* = 1.0, *convfact* = 1.1, and *conv_nregions* = 2. Convergence checking was initiated immediately at the 62 region point (*chk_nregions* = 62).

Major jumps in *dval* and *max_threshold* were noticed between hierarchical level 11 (42 regions, *dval* = 0.480455 and *max_threshold* = 63.249) and hierarchical level 12 (10 regions, *dval* = 1.63727 and *max_threshold* = 2503.99). RHSEG was then rerun with *chk_nregions* = 10, and the 10 region segmentation was inspected with the *HSEGViewer* visualization tool.

In this case the trace and resonance regions are not clearly delineated. Fig. 6 shows the 10 region segmentation result, color coded using *HSEGViewer* to look similar to the pseudo colored plasmagram data as shown in Fig. 5. Regions 4, 5 and 10 make up the blue background region. Regions 6 and 9 make up the tourquoise region, which is a mix of background resonances and plasma trace (especially at the higher frequencies). Regions 7 and 8 make up the dark green region, and region 3 makes up the light green region. These regions are mostly background at the lower frequencies, but include some resonance and trace signals at the higher frequencies. Region 2 is colored orange, and consists primarily of the strongest trace and resonance signals. The yellow colored region 1 consists primarily of the more moderate trace and resonance signals.

In studying plasmagram 20010917_032244 in the previous section, the next step was to create a mask from the regions covering most of the trace and resonance signals. However, the results here are too mixed to do this. Some preprocessing might be useful in cleaning up the results. Perhaps subtracting the minimum, mean or median values from the signal at each frequency would more cleanly delineate the trace signals (of course, this would obliterate the resonance signals). This would even help the analysis in the cleaner plasmagram 20010917_032244 of the previous section. Note that a couple of the trace signals are split into subregions in Fig. 4 (note the pink and red subregions for one trace and the light green and dark green subregions for another trace). The subregions arise because the background adds to the signal, and the background varies with frequency. Subtracting the minimum, mean or median value should serve to make the trace values appear more similar along the entire length of the trace, which would make it more likely the whole trace will be seen as one region by RHSEG. This preprocessing should have the same effect for plasmagram 20010118_023716. The result of testing this type of preprocessing should be available for the conference presentation.

VI. Summary

An increasing number of the Earth observing programs spawn the intelligent system applications to establish an automated clearinghouse for dispersed and disorganized data. The computer plays an especially powerful and enabling role in those projects where the dataset size precludes manual processing. Our work was inspired by the practical need of locating scientifically-significant data records in the large archive of IMAGE/RPI plasmagrams, snapshots of plasma conditions in the Earth's magnetosphere. Less that 4% of nearly 900,000 collected plasmagram images have been manually analyzed. We developed an automated data exploration tool, CORPRAL, to locate, sort and pre-classify plasmagrams containing traces of remote reflections of the RPI signal. CORPRAL uses a biologically plausible model of pre-attentive vision replicating the key components of low-level, bottom-up analysis in retina and brain cortex. Exploring the plasmagram archive with CORPRAL yielded almost 150,000 plasmagrams with traces (~17% of all data). We plan to seek further enhancements of the CORPRAL by bringing its design closer to the bio-plausible solutions developed over the million years of evolution. This paper discussed a particular problem of false-alarm rate caused by imperfections of the edge analysis in CORPRAL. We look into higher

complexity 2D techniques to analyze echo integrity across the plasmagram images and thus help to bring down the false positive decisions. HSEG method for hierarchical segmentation of visual information is a well established technique developed for a broad class of remotely-sensed images. The RHSEG implementation of the segmentation technique demonstrates good potential for this task. We are working on developing shape descriptors for the RHSEG technique that would allow constrained clustering to find elongated regions corresponding to the plasmagram traces.

REFERENCES

[1] B. W. Reinisch, et al, "The Radio Plasma Imager investigation on the IMAGE spacecraft," *Space Science Reviews*, vol. 91, 2000, pp. 319-35.

[2] J. L. Burch (ed), *The IMAGE Mission*. Dordrecht: Kluwer Acad. Pub., 2000, 506 pp.

[3] Ivan A. Galkin., Bodo W. Reinisch, Xueqin Huang, Robert F. Benson, and Shing F. Fung , "Automated diagnostics for resonance signature recognition on IMAGE/RPI plasmagrams," *Radio Science*, 39, 1, RS1015, 10.1029/2003RS002921, Feb. 24, 2004.

[4] I. A. Galkin, B.W. Reinisch, G. Grinstein, G. Khmyrov, A. Kozlov, and S. F. Fung, "Automated exploration of the Radio Plasma Imager data," unpublished.

[5] J. C. Tilton, "Analysis of hierarchically related image segmentations," *Proc. IEEE Workshop on Advances in Techniques for Analysis of Remotely Sensed Data*, Greenbelt, MD, USA, October 27-28, 2003.

[6] J. C. Tilton, "Hierarchical image segmentation by recursive hierarchical step-wise optimization and constrained spectral clustering," in preparation for submission to the *IEEE Transactions on Image Processing*.

[7] J-M. Beaulieu and M. Goldberg, "Hierarchy in picture segmentation: A stepwise optimal approach," *IEEE Transactions on Pattern Analysis and Machine Intelligence*, Vol. 11, No. 2, pp. 150-163, Feb. 1989.

[8] J. C. Tilton, "A method for recursive hierarchical segmentation which eliminates processing window artifacts," *Disclosure of Invention and New Technology (Including Software): NASA Case No. GSC 14,681-1 (revised)*, NASA's Goddard Space Flight Center, Jan. 24, 2003.

[9] Reinisch, , X. Huang, Haines, I. A. Galkin, Green, Benson, Fung , Taylor, Reiff, Gallagher, Bougeret, Manning, and Carpenter, First Results from the Radio Plasma Imager on IMAGE, *Geophys. Res. Letts*., **28**, 1167-1170, 2001.

[10] Carpenter, D. L., M. Spasojevic, T. F. Bell, U. S. Inan, B. W. Reinisch, I. A. Galkin, R. F. Benson, J. L. Green, S. F. Fung, S. A. Boardsen, Small-scale field-aligned plasmaspheric density structures inferred from RPI on IMAGE, 107(A9), 1258, *J. Geophys. Res*., 2002.

[11] Fung, S. F., Benson, R.F., Green, J.L., Reinisch, B.W., Haines, D.M., Galkin, I. A., Bougeret, J.-L., Manning, R., Reiff, P.H., Carpenter, D.L., Gallagher, D.L., and Taylor, W.W.L., Observations of Magnetospheric Plasmas by the Radio Plasma Imager (RPI) on the IMAGE Mission, *Adv. Space Res*., 30 (10), 2259-2266, 2002

[12] Fung, S. F., R. F. Benson, D. L. Carpenter, J. L. Green, V. Jayanti, I. A. Galkin, and B. W. Reinisch, Guided echoes in the magnetosphere: Observations by Radio Plasma Imager on IMAGE, *Geophys. Res. Lett*., 30(11), 1589, 2003

[13] Nsumei, P.A., Huang, X., Reinisch, B.W., Song, P., Vasyliunas, V.M., Green, J.L., Fung, S.F., Benson, R.F., and Gallagher, D.L., Electron Density Distribution Over the Northern Polar Region Deduced from IMAGE/RPI Sounding, *J. Geophys. Res*., 108, A2, 2003.

[14] Rock, I., and S. Palmer, The legacy of Gestalt psychology, *Sci. American*, *SCA9012*, 84-90, 1990.

[15] Galkin, I.A., G. M. Khmyrov, A. Kozlov, B.W. Reinisch, X. Huang, and G. Sales, New tools for analysis of space-borne sounding data, Proc. 2001 USNC/URSI Nat. Radio Sci. Meeting, Boston, MA, 304, 2001.

[16] Marr, D., and H.K. Nishihara, Visual information processing: Artificial intelligence and the sensorium of light, *Technology review*, **81**, 2-23, 1978